water

MDPI

Article

Investigating the Influence of the Relative Roughness of the Riverbanks to the Riverbed on Equilibrium Channel Geometry in Alluvial Rivers: A Variational Approach

Jinsheng Fan [1,2,*], Qiushi Luo [1,2], Yuchuan Bai [3], Xiaofang Liu [4] and Renzhi Li [5]

1 Yellow River Engineering Consulting Co., Ltd., Zhengzhou 450003, China; luoqiushi@163.com
2 Key Laboratory of Water Management and Water Security for Yellow River Basin, Ministry of Water Resources (Under Construction), Zhengzhou 450003, China
3 Institute for Sediment, River and Coast Engineering, Tianjin University, Tianjin 300072, China; ychbai@tju.edu.cn
4 Beijing Capital Ecological Environmental Protection Group Co., Ltd., Beijing 100044, China; liuxf.11b@igsnrr.ac.cn
5 National Institute of Natural Hazards, Ministry of Emergency Management of the People's Republic of China, Beijing 100085, China; renzhili@ninhm.ac.cn
* Correspondence: fanjs.16b@igsnrr.ac.cn; Tel.: +86-130-0127-6557

Abstract: The roughness of a river's boundary significantly influences the sediment transport process and the ultimate configuration of the river's stable cross-section. This interplay between boundary roughness and river morphology is crucial to a river's overall behavior and form. This study aims to analyze the influence of the relative roughness of riverbanks to a riverbed λ on the equilibrium form of alluvial rivers using a variational method. The results show the following: (1) As the parameter λ transitions from smaller to larger values, noteworthy variations are observed in a river's characteristics. Specifically, there is a discernible reduction in the calculated maximum sediment discharge, coupled with a corresponding expansion in the optimal width–depth ratio. For instance, when λ changes from 1 to 0.1, the optimal width–depth ratio increases by 45%, while the calculated maximum sediment discharge experiences a decrease of 1.62%. (2) An examination of hydraulic geometric relationships, derived by assigning distinct values to the relative roughness of riverbanks to the riverbed, highlights the significant influence of this relative roughness on the ultimate equilibrium configuration of the river channel. Remarkably, this effect remains consistent and stands independently of other variables such as sediment discharge, flow discharge, channel gradient, and sediment size. (3) The critical and average hydraulic geometric relationships deduced in this study closely align with previous research findings. Notably, this research contributes to addressing the existing gap in understanding the mechanistic underpinnings of how river boundary conditions impact the equilibrium forms of rivers, thereby advancing our knowledge of river morphology. Nevertheless, it is imperative to emphasize that while this study provides valuable theoretical insights, the practical application of these findings in the context of river morphological evolution necessitates further in-depth research. It calls for a more comprehensive exploration of the transition from theoretical constructs to real-world applications, thus promoting a deeper understanding of the dynamics that shape river systems.

Keywords: relative roughness; riverbanks; riverbed; variational method; river morphology; alluvial rivers

check for updates

Citation: Fan, J.; Luo, Q.; Bai, Y.; Liu, X.; Li, R. Investigating the Influence of the Relative Roughness of the Riverbanks to the Riverbed on Equilibrium Channel Geometry in Alluvial Rivers: A Variational Approach. *Water* **2023**, *15*, 4029. https://doi.org/10.3390/w15224029

Academic Editor: Achim A. Beylich

Received: 22 October 2023
Revised: 11 November 2023
Accepted: 14 November 2023
Published: 20 November 2023

1. Introduction

As complex natural systems, rivers inherently exhibit the capacity to self-regulate and attain a dynamic equilibrium state. This dynamic equilibrium state is characterized by a delicate balance between erosional and depositional processes, achieved through the river's ability to adjust its channel geometry and gradient [1,2]. Dynamic equilibrium in

river systems is paramount in fluvial geomorphology and river engineering. It serves as the linchpin for understanding the intricate and multifaceted interactions among various factors, including river flow dynamics, sediment transport mechanisms, and the resultant morphological features of the river channel. While rivers have the innate propensity to operate within a state of dynamic equilibrium, certain conditions and external factors can lead to temporary deviations from this equilibrium state.

Nevertheless, the dynamic equilibrium state is a guiding principle, akin to an overarching attractor, influencing the natural adjustments in river channel forms [3]. These adjustments are a testament to a river's innate capacity to respond to changing environmental conditions and balance erosion and deposition. In recent decades, rivers worldwide have encountered substantial anthropogenic interventions, ranging from riverbank reinforcement to dam construction, urban expansion into floodplains, agricultural development, and logging practices, among others [4]. The cumulative impact of these interventions on river systems raises crucial questions. Assessing the extent to which these human activities have caused deviations from the state of dynamic equilibrium within river systems becomes imperative. Equally vital is whether these rivers still retain the inherent capability to return to a state of dynamic equilibrium. Determining the dynamic equilibrium state in river channel flow transcends mere academic curiosity. It enriches our understanding of river behavior and the underlying physical processes governing their responses to environmental changes [5]. Furthermore, this understanding provides invaluable guidance for developing effective strategies to preserve and restore river systems [6]. By comprehending the complex interplay of factors influencing rivers and their dynamic equilibrium, we can better navigate the challenges posed by contemporary human activities and work toward sustainable river management and conservation.

In specific hydrological conditions characterized by distinct flow discharge, sediment discharge, and erodible boundaries, rivers have the remarkable capacity to adjust their channel characteristics, such as width, depth, and gradient. These adjustments enable a river to transport sediment from its upstream regions, culminating in a dynamic equilibrium state where neither erosion nor deposition prevails [2]. Dynamic equilibrium in river systems has been a subject of scientific inquiry for many years. Early investigations in this domain predominantly relied on empirical approaches, resulting in qualitative descriptions and the development of quantitative statistical hydraulic geometric relationships [7–10]. Despite the contributions of these empirical studies, which provided valuable insights into river equilibrium dynamics, they have remained limited in elucidating the intricate internal physical mechanisms governing the evolution of river systems [11]. While qualitative descriptions and quantitative hydraulic geometric relationships have proven beneficial in characterizing river behavior and morphology, they have offered little to explicate the underlying physical processes that drive river channel adjustments [12–17]. As such, a substantial gap exists in our understanding of the fundamental mechanisms at play during the evolution of river systems. This gap necessitates a more comprehensive and mechanistic exploration of the internal dynamics governing the dynamic equilibrium state in rivers.

In light of the complexities surrounding river equilibrium dynamics, contemporary research endeavors aim to transcend the limitations of past empirical approaches. Instead, they seek to unravel the intrinsic physical mechanisms responsible for shaping river channel forms. By delving deeper into the internal workings of rivers, the scientific community strives to elucidate the intricate interactions between flow dynamics, sediment transport, and the evolution of river channels. This evolving scientific discourse is driven by a commitment to uncover the underlying principles that govern the dynamic equilibrium state in river systems, thereby providing a more robust and comprehensive understanding of these vital natural entities.

The endeavor to comprehensively elucidate the evolutionary processes governing rivers encounters an inherent challenge—a seemingly inescapable conundrum marked by three fundamental relationships characterizing river flow and four unknown variables. This intricate system, bereft of a closed-form solution, necessitates innovative approaches

for resolution [18]. Numerous theoretical frameworks have been introduced to surmount this challenge, notably stability and extreme hypothesis theories. The stability theory posits the notion of river stability, implying that sediment throughout the entirety of a river boundary is perpetually in a critical incipient motion state [19,20]. While the stability theory provides a highly rigorous and theoretically sound foundation for understanding river dynamics, it is not without its limitations, particularly in scenarios where achieving satisfactory computational results remains elusive [21]. The capacity of the stability theory to offer precise predictions is subject to constraints in certain situations, prompting the exploration of alternative methodologies to address this shortcoming.

Much like stability theories, the extremal hypotheses approach seeks to introduce an extremal condition as an additional flow equation, with examples encompassing parameters like a minimum energy gradient [22–29], maximum sediment transport capacity [30], and minimum energy loss rate [31–39], among others. While this approach offers relative ease of application, its utilization has stirred significant debate within the scientific community. Critics of the extremal hypothesis methodology raise two primary objections: firstly, a river channel's width computed using extremal hypotheses consistently falls short of observed measurements and secondly, it is contended that extremal hypotheses lack robust physical mechanisms to justify their adoption [40,41]. Conversely, proponents of extremal hypotheses posit that these theories are grounded in widely applicable physical principles, such as the principles of minimum work and maximum entropy [42–44]. Additionally, some argue that the detractors have employed the extremal approach incompletely, failing to account for the influence of riverbank anti-scourability on river channel morphology [40, 41,45]. Building upon a series of investigations, Eaton and Millar introduced the UBC model, incorporating the repose angle of a bank sediment into their extremal hypothesis-based framework. This integration enabled the UBC model to better encapsulate the effects of riverbank anti-scourability, resulting in improved computational accuracy in predicting alluvial channel forms across various scenarios [46]. The discourse surrounding extremal hypotheses in river dynamics remains a topic of substantial complexity and divergence of opinion, with ongoing research endeavors aiming to reconcile contrasting viewpoints and develop more comprehensive models that accommodate the intricacies of river channel behavior. This pursuit is instrumental in furthering our comprehension of river equilibrium and evolution, enhancing the efficacy of river engineering and preservation efforts.

In a departure from the equilibrium models, such as the stability theory and the extreme hypothesis, a novel approach was introduced by Huang and collaborator Nanson [47–50], known as the variational model. This model aimed to streamline the computational process and reduce the number of unknown variables by introducing the variational factor ζ = W/D (width/depth ratio). Doing so effectively addressed the fundamental flow equations governing river systems. The variational analysis model revealed that the maximum sediment transport rate and the minimum channel slope characterize the optimal hydraulic conditions for achieving the most favorable river channel morphology. Importantly, it established that these conditions are specific manifestations of the principle of least action, a well-established physics concept applied to river systems. In essence, alluvial rivers exhibit two primary modes for achieving optimal sediment transport: for a given discharge and sediment transport rate, channel morphology is adjusted to minimize the slope, whereas for a given flow discharge and slope, channel morphology is adjusted to maximize the sediment transport rate. Huang's variational model has proven to be instrumental in elucidating the evolution of river morphology and explaining the formation mechanisms of various river patterns. Additionally, recent research by Fan and Huang in 2020 extended this model by incorporating bank steepness as a factor to partially reflect the anti-scourability of riverbanks, further enhancing its utility in understanding and analyzing river systems [51].

However, the concept of river boundary conditions is multifaceted, and bank steepness alone may not comprehensively capture an entire riverbank's anti-scourability. Thus, a pressing need arises to investigate additional factors contributing to the anti-scourability

of riverbanks to gain deeper insights into the evolutionary processes shaping river geomorphology. Consequently, this study delves into the examination of the relative roughness of riverbanks to a riverbed, which represents another pivotal aspect of river boundary anti-scourability. In this endeavor, we employed a rectangular shape as a generalized cross-section of a river, providing an in-depth analysis of how this parameter influenced the ultimate equilibrium form of the river. Moreover, we deduced the critical and average hydraulic geometric relationships under varying degrees of the relative roughness of riverbanks to a riverbed. These deduced relationships were subsequently scrutinized for consistency with prior theoretical analyses and empirical findings. This exploration into the relative roughness of riverbanks to a riverbed constitutes a crucial step toward enhancing our understanding of river geomorphology and advancing our knowledge of the intricate interplay between hydraulic factors and boundary anti-scourability in the context of river systems.

2. Methodology

2.1. Huang's Variational Model

In the context of straight and single-thread alluvial open channels with a rectangular cross-section, the research conducted by Huang and Nanson (2000, 2002) and Huang et al. (2004) presents a noteworthy contribution [47–49]. Their analytical investigations unveiled a profound revelation—establishing a curvilinear equilibrium relationship. This relationship provides insights into the intricate dynamics between Q_s, representing the bedload transport discharge within a channel, and ζ, which denotes the channel's cross-sectional shape factor, specifically its width-to-depth ratio.

This equilibrium relationship is of paramount significance as it elucidates the existence of a specific width-to-depth ratio, referred to as ζ_m, which corresponds to the maximum bedload transport discharge point, Q_{smax}. This maximum discharge point is achieved under well-defined flow energy conditions, encompassing a flow discharge and an energy gradient, as well as the channel's boundary composition, particularly related to sediment size. The implications of this relationship are significant, shedding light on the complex dynamics governing bedload transport in alluvial open channels.

It is essential to emphasize that the curvilinear relationship between the bedload transport discharge (Q_s) and the width-to-depth ratio (ζ) offers a comprehensive portrayal of the underlying dynamics. When the bedload transport discharge reaches its maximum value, denoted as $Q_s = Q_{smax}$, under specific conditions comprising flow discharge, energy slope and sediment size, a unique value for the width-to-depth ratio, ζ_m, emerges. This specific state is known as maximum flow efficiency (MFE), a term introduced by Huang and Nanson [51]. In cases where the bedload transport discharge is less than the maximum, i.e., $Q_s < Q_{smax}$, a single value for bedload transport discharge can be achieved through two distinct width-to-depth ratios, one smaller and the other larger than ζ_m. In the broader framework of physics, MFE signifies the state of stationary equilibrium in river channel flow. It embodies the concept of the most efficient utilization of available energy by the flow for transporting a given bedload, resulting in the maximum bedload discharge while expending the specified energy quantity. In contrast, the other states represent dynamic equilibrium states, wherein the flow has the flexibility to choose between two channel cross-sections. These cross-sections offer varying resistance levels, allowing for the expenditure of more than the minimal energy required. These concepts were further elucidated by Huang et al. (2004) and Nanson and Huang (2008) [4,48].

2.2. Definition of the Relative Roughness of Riverbank to the Riverbed

The boundary conditions of alluvial rivers exhibit significant variability, particularly concerning the roughness of riverbanks relative to a riverbed. This variability results in a diverse range of river morphologies. This study explores the impact of the relative roughness of riverbanks to a riverbed on the equilibrium channel configuration of alluvial rivers. It employs a simplified rectangular cross-section for representing a river [3–6,51–53],

as depicted in Figure 1. The factor influencing the relative roughness of the riverbank to the riverbed was incorporated using the hydraulic radius segmentation method. Variational analysis was employed to assess its influence on the equilibrium channel shape of a river.

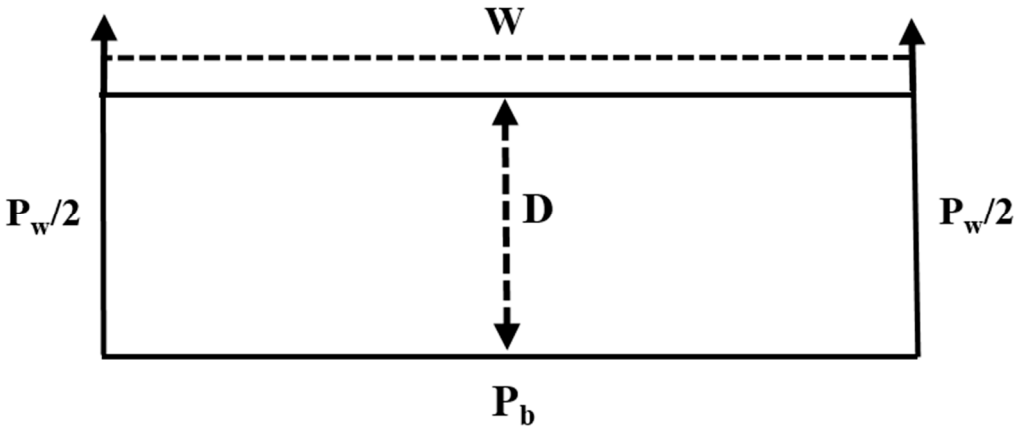

Figure 1. Overview of river flow cross-section.

For a one-dimensional flow continuity equation, the formula is given as the following:

$$Q = VA \tag{1}$$

In Equation (1), Q expresses flow discharge, V represents flow velocity, and A means a cross-sectional area.

For the resistance equation of alluvial rivers, the Manning formula was adopted in this paper, as shown in the following formula [52]:

$$V = \frac{1}{n} R^{2/3} S^{1/2} \tag{2}$$

In Equation (2), n expresses the roughness coefficient, R represents the hydraulic radius, and S means the channel slope.

The bedload transport equation adopted in this paper is expressed as the exponential form of shear force, shown as the following [53,54]:

$$q_b = c_b \tau_0^i (\tau_0 - \tau_c)^j \tag{3}$$

In Equation (3), q_b expresses the bedload transport rate on the unit width, c_b represents a coefficient, τ_0 means the average shear stress ($\tau_0 = \gamma \mathrm{RS}$), and τ_c means the critical shear stress for the critical starting state of the sediment.

However, it has been proven that the following formula is closer to the natural sediment transport condition of a river under many conditions:

$$q_b^* = c_b (\tau_0^* - \tau_c^*)^j \tag{4}$$

In Equation (4), q_b^* expresses the dimensionless rate of bedload transport on the unit width, τ_0^* represents dimensionless average flow shear stress, and τ_c^* means dimensionless critical flow shear stress, which separately is expressed as the following:

$$\begin{gathered} q_b^* = \frac{q_b}{\sqrt{(\gamma_s/\gamma - 1) g d^3}} = \frac{Q_s / P_b}{\sqrt{(\gamma_s/\gamma - 1) g d^3}} \\ \tau_0^* = \frac{\tau_0}{(\gamma_s - \gamma) d} = \frac{\gamma R S}{(\gamma_s - \gamma) d} \\ \tau_c^* = \frac{\tau_c}{(\gamma_s - \gamma) d} \end{gathered} \tag{5}$$

In Equation (5), P_b means the wetted perimeter of the cross-section, Q_s represents the bedload transport discharge, γ_s means the specific weight of sediment particles ($\gamma_s = \rho_s g$),

γ is the specific weight of water ($\gamma = \rho g$), ρ_s expresses the density of sediment particles (2650 kg/m^3), ρ means the density of water (1000 kg/m^3), and g means the gravity acceleration (9.8 m/s^2).

Furthermore, in previous studies [53,54], the values of c_b, τ_c^*, and j have been different. In this study, since the research method inherits the equilibrium theory of Huang, the research results of Huang (2010) were adopted [50], in which j = 5/3, c_b = 6, and τ_c^* = 0.047. Therefore, Formula (4) can be simplified to the following form:

$$q_b^* = 6(\tau_0^* - 0.047)^{5/3} \tag{6}$$

To evaluate the impact of the non-uniform distribution of riverbed boundary roughness on channel morphology, Einstein suggested employing the hydraulic radius segmentation method for partitioning boundary resistance [55,56]. This method integrates the Manning formula for channel resistance segmentation. The specific formulation is the following:

$$(n)^{3/2}P = (n_b)^{3/2}P_b + (n_w)^{3/2}P_w \tag{7}$$

where n, n_b, and n_w are, respectively, the comprehensive roughness coefficient of the whole cross-section, the roughness coefficient of the riverbed, and the roughness coefficient of the riverbank, and P, P_b, and P_w are the wetted perimeter of the whole cross-section, the riverbed, and the riverbank, respectively.

For the channel with a rectangular cross-section, as shown in Figure 1, the following geometric relationship exists as

$$P = W + 2D,\ P_b = W,\ P_w = 2D \tag{8}$$

where W and D are, respectively, the width of the river and the depth of the river. Accordingly, Equation (7) can be specifically expressed as the following:

$$(n)^{3/2}(\mathrm{W} + 2\mathrm{D}) = (n_b)^{3/2}\mathrm{W} + (n_w)^{3/2}2\mathrm{D} \tag{9}$$

The relative roughness of riverbanks to a riverbed is represented by the variable λ, and the definition is the following:

$$\lambda = (n_w)^{3/2}/(n_b)^{3/2} \tag{10}$$

3. Mathematical Analysis of the Influence of Relative Roughness of Riverbanks to a Riverbed on River Channel Equilibrium Form

In accordance with the river equilibrium theory and the variational method developed by Huang and his collaborators [3–6,51–53], in order to reduce the number of unknown variables, it is necessary to combine river width and depth into a single variable, as illustrated in Figure 1. This newly combined variable is expressed as the following:

$$\zeta = \frac{W}{D} \tag{11}$$

In Equation (11), W expresses the width of the channel and D represents the depth of the channel.

For the river cross-section shown in Figure 1, there is the following basic geometric relationship:

$$R = \zeta(\zeta + 2)^{-1}D \tag{12}$$

Combining Equations (1), (2), (7), and (8) yields the following relationships:

$$\begin{aligned} W &= (nQ)^{3/8}S^{-3/16}(\zeta + 2)^{1/4}\zeta^{3/8} \\ D &= (nQ)^{3/8}S^{-3/16}(\zeta + 2)^{1/4}\zeta^{-5/8} \\ \tau_0 &= \gamma(nQ)^{3/8}S^{13/16}(\zeta + 2)^{-3/4}\zeta^{3/8} \end{aligned} \tag{13}$$

In order to reflect the influence of the uneven distribution of boundary roughness, combining Equations (7), (8), (11), and (12) yields the following relationship:

$$n^{3/2} = \frac{(\zeta + 2\lambda)}{\zeta + 2} n_b^{3/2} \tag{14}$$

Incorporating Equation (14) into (13) yields the following relations:

$$\begin{aligned} W &= (n_b Q)^{3/8} S^{-3/16} (\zeta + 2\lambda)^{1/4} \zeta^{3/8} \\ D &= (n_b Q)^{3/8} S^{-3/16} (\zeta + 2\lambda)^{1/4} \zeta^{-5/8} \\ \tau_0 &= \gamma (n_b Q)^{3/8} S^{13/16} (\zeta + 2\lambda)^{1/4} (\zeta + 2)^{-1} \zeta^{3/8} \end{aligned} \tag{15}$$

Combining Equations (5), (6), and (15) with $Qs = q_b W$ yields the following:

$$Q_s = K_0 (\zeta + 2\lambda)^{1/4} \zeta^{3/8} \left[K_1 \frac{(\zeta + 2\lambda)^{1/4} \zeta^{3/8}}{(\zeta + 2)} - 0.047 \right]^{5/3} \tag{16}$$

where constants K_0, K_1, and λ are determined by the following equations:

$$\begin{aligned} K_0 &= 24.1275 d^{3/2} (n_b Q)^{3/8} S^{-3/16}; \\ K_1 &= \frac{\gamma (n_b Q)^{3/8} S^{13/16}}{(\gamma_s - \gamma) d}; \end{aligned} \tag{17}$$

Utilizing Formulas (16) and (17), where Q was set to 4000 cubic meters per second, the channel gradient was 2/10,000, sediment size (d), was 0.6 mm, and roughness, was 0.012; variable λ was assigned values of 0.1, 0.5, 1, and 2 to represent different relative roughness of riverbanks to a riverbed. Subsequently, a curve of Q_s was generated concerning ζ within the range of 10–1000. Figure 2 and Table 1 display the variation curve and computation results of sediment discharge, respectively.

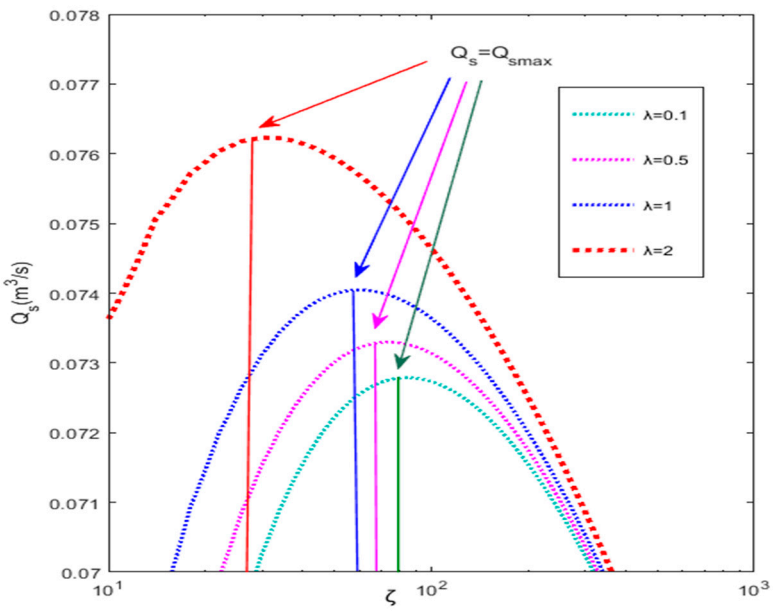

Figure 2. Relationship between Q_s and ζ for different values of λ.

It is evident from Figure 2 that as the relative roughness of riverbanks to a riverbed varies, the sediment discharge curve takes the shape of a parabola with a downward opening. It initially rises slowly, reaches its peak at a certain point, and then descends gradually. Notably, there is only one eligible width–depth ratio corresponding to the peak point along the curve. Conversely, for points on the curve that are less than the peak value,

two corresponding width–depth ratios are available. For points greater than the peak, there is either no corresponding width–depth ratio or no solution.

Table 1. Values of Q_{smax} and ζ_m under different values of λ.

λ	ζ_m	$\frac{\zeta_m - \zeta_{m0}}{\zeta_{m0}}$ (%)	Q_{smax} (m^3/s)	$\frac{Q_{smax} - Q_{smax0}}{Q_{smax0}}$ (%)
1	61.48	0	0.0741	0
0.1	89.2	45.09	0.0729	−1.62
0.5	73.36	19.32	0.0734	−0.94
2	29.8	−51.53	0.0763	2.97

Furthermore, when the relative roughness of riverbanks to a riverbed was set at values of 0.1, 0.5, 1, and 2, the apex of the $Q_{s\max}$ curve increased as the values grew larger. Specifically, the corresponding $Q_{s\max}$ values for each level of relative roughness were 0.0729, 0.0734, 0.0741, and 0.0763, respectively. Conversely, the associated width–depth ratio at the highest point ζ_m decreased with larger relative roughness values, measuring 89.2, 73.36, 61.48, and 29.8, respectively.

To quantify the influence of changes in the relative roughness of a riverbank to a riverbed on both sediment discharge and width–depth ratio, using a reference level of a relative roughness value of 1, we observed from Table 1 that when the relative roughness was 0.1, 0.5, and 2, the width–depth ratio changed by −51.53%, 19.32%, and 45.09%, respectively. Simultaneously, the sediment discharge experienced changes of −1.62%, −0.94%, and 2.97%, respectively. These data illustrate that the alteration in the relative roughness of a riverbank to a riverbed has a more pronounced effect on the width–depth ratio compared to its impact on sediment discharge.

Assuming n_b, Q, S, and λ are constants, the following relationships can be obtained by differentiating ζ on both sides of Formula (15):

$$\begin{gathered} \frac{1}{D}\frac{dD}{d\zeta} = -\frac{-3\zeta-10\lambda}{8\zeta(\zeta+2\lambda)} \\ \frac{1}{W}\frac{dW}{d\zeta} = \frac{5\zeta+6\lambda}{8\zeta(\zeta+2\lambda)} \\ \frac{1}{\tau_0}\frac{d\tau_0}{d\zeta} = \frac{-3\zeta^2+10\zeta-10\lambda\zeta+12\lambda}{8\zeta(\zeta+2)(\zeta+2\lambda)} \end{gathered} \tag{18}$$

Using the bedload sediment discharge expression as shown in Formula (3), the derivation of ζ on both sides of the Formula (3) was obtained, which is expressed as the following:

$$\frac{1}{Q_s}\frac{dQ_s}{d\zeta} = \frac{1}{W}\frac{dW}{d\zeta} + \left(i + \frac{\tau_0 j}{\tau_0 - \tau_c}\right)\frac{1}{\tau_0}\frac{d\tau_0}{d\zeta} \tag{19}$$

According to the differential principle, when the function value reaches the maximum, the differential of the function value to the variable equals 0. Therefore, an equation can be derived as the following:

$$\frac{dQ_s}{d\zeta} = 0 \tag{20}$$

The following equations can be obtained by solving Equations (18)–(20) simultaneously:

$$\frac{\tau_0}{\tau_c} = \frac{A + Bi}{A + B(i + j)} \tag{21}$$

In relationship (21), parameters A and B can be expressed as the following forms:

$$\begin{gathered} A = 5\zeta^2 + 6\lambda\zeta + 10\zeta + 12\lambda \\ B = -3\zeta^2 + 10\zeta - 10\lambda\zeta + 12\lambda \end{gathered} \tag{22}$$

In order to be consistent with Huang's research, Formula (6) was adopted as the bedload transport rate formula, i.e., i is equal to 0 and j is equal to 5/3, so Equation (21) can be simplified as the following:

$$\frac{\tau_0}{\tau_c} = \frac{A}{A + (5/3)B} \tag{23}$$

Through mathematical transformation, Equation (23) can be simplified into the following form:

$$\frac{\tau_0 - \tau_c}{\tau_c} = \frac{-(5/3)B}{A + (5/3)B} \tag{24}$$

Furthermore, it can be seen from Formula (24) that based on the differential principle, when the sediment discharge reaches the maximum at the lower threshold, it needs to meet the condition of $\tau_0 = \tau_c$, i.e., $B = 0$. By solving equation $B = 0$, as expressed in Equation (22), the solutions can be obtained as the following:

$$\zeta_{mc} = \frac{10(1-\lambda) \pm \sqrt{100(1-\lambda)^2 + 144\lambda}}{6} \tag{25}$$

As can be seen from Formula (25), there are two values that can satisfy $B = 0$, but only $\zeta_{mc} = [10(1-\lambda) + \sqrt{100(1-\lambda)^2 + 144\lambda}]/6$ is a reasonable solution, which is inconsistent with actual river conditions. In particular, when $\lambda = 1$, $\zeta_m = 2$, it is 100% consistent with Huang's previous research [51], which further proves the rationality of the reasoning process used in this paper. Therefore, the reasonable solution in the case of a low threshold of $\tau_0 = \tau_c$ can be expressed as

$$\zeta_{mc} = \frac{10(1-\lambda) + \sqrt{100(1-\lambda)^2 + 144\lambda}}{6} \tag{26}$$

4. Effects of Relative Roughness of Riverbanks to a Riverbed on Equilibrium Hydraulic Geometry

4.1. Equilibrium Hydraulic Geometry in the State of $\tau_0 = \tau_c$

Under the assumption that the sediment on a riverbed has reached a critical incipient motion state, i.e., $\tau_0 = \tau_c$, the critical hydraulic geometric expression can be derived by concurrently solving Formulas (13) and (26):

$$\begin{aligned} W &= aQ^{6/13} \\ D &= bQ^{6/13} \\ S &= cQ^{-6/13} \end{aligned} \tag{27}$$

In relationships (27), the correlation coefficients a, b, and c are determined by the following relationships:

$$\begin{aligned} a &= c^{-3/16} n^{3/8} (\zeta_m + 2)^{1/4} \zeta_m^{3/8} \\ b &= c^{-3/16} n^{3/8} (\zeta_m + 2)^{1/4} \zeta_m^{-5/8} \\ c &= [0.047 \tfrac{(\gamma_s - \gamma)d}{\gamma n^{3/8}} (\zeta_m + 2)^{3/4} \zeta_m^{-3/8}]^{16/13} \end{aligned} \tag{28}$$

Building upon the framework established by Formula (28), we introduced specified parameters, setting variable n at 0.03, d at 0.3 mm, ρ_s at 2650 kg/m^3, and ρ at 1000 kg/m^3. Subsequently, we varied the coefficient λ across values of 0.1, 0.5, 1, and 2 to represent the changing relative roughness of riverbanks to a riverbed. Analysis of the results presented in Table 2 demonstrated that as λ transitioned from lower to higher values, coefficients a, b, and c exhibited distinct variations within a narrow range. In more precise terms, with λ values of 0.1, 0.5, 1, and 2, a assumed the respective values of 4.4642, 3.9633, 3.7919,

and 3.6405, while b took on values of 1.4266, 1.6015, 1.8960, and 2.2524. The coefficient c registered values of 2.6736×10^{-5}, 2.6267×10^{-5}, 1.8698×10^{-5}, and 1.3268×10^{-5}. Notably, as λ increased, a gradually decreased, while b steadily increased. This implies that in scenarios where a river operates under a lower threshold state, a smaller λ value leads to adopting a narrower and deeper cross-sectional configuration for sediment transport.

Table 2. Values of the coefficients a, b, and c under different values of λ.

λ	ζ_m	Values of a, b, and c
0.1	3.12	$a = 4.4622$ $b = 1.4266$ $c = 2.6736 \times 10^{-5}$
0.5	2.47	$a = 3.9633$ $b = 1.6015$ $c = 2.6267 \times 10^{-5}$
1	2	$a = 3.7919$ $b = 1.8960$ $c = 1.8698 \times 10^{-5}$
2	1.62	$a = 3.6405$ $b = 2.2524$ $c = 1.3268 \times 10^{-5}$

4.2. Averaged Equilibrium Hydraulic Geometry at the State of $\tau_0 > \tau_c$

Formulas (23) and (24) reveal that the width–depth ratio variable, as dictated by Formula (20), can span any positive range of values. A series of mathematical transformations must be applied to derive the geometric relationship for average river hydraulic characteristics. Consequently, Equations (11)–(13), (22), and (23), and the condition $Q_s = q_b P_b = q_b W$, were simultaneously solved to eliminate the variable energy gradient S. Through this process, the relationships among the optimal width–depth ratio, variable flow discharge, sediment discharge, sediment size, the relative roughness of riverbanks to a riverbed, and roughness were ascertained as the following:

$$\left(\frac{-(5/3)B}{A+(5/3)B}\right)^{65/9} \frac{A+(5/3)B}{A} {\zeta_m}^2 (\zeta_m + 2)^{1/3} = 3.0725 * 10^2 d^{-11/2} \frac{Q_s^{13/3}}{(nQ)^2} \tag{29}$$

Consequently, Equation (29) was combined with Equations (12), (13), (22), and (23) to express the equilibrium channel slope S_m, width W_m, and depth D_m as

$$S_m = \left(\frac{-(5/3)B}{A+(5/3)B}\right)^{80/9} {\zeta_m}^2 (\zeta_m + 2)^{4/3} = 3.7136 * 10^{-5} d^8 \frac{(nQ)^2}{Q_s^{16/3}} \tag{30}$$

$$W_m = \frac{Q_s}{1.4768 * 10^{-1} d^{3/2} \left(\frac{-(5/3)B}{A+(5/3)B}\right)^{5/3}} \tag{31}$$

$$D_m = \frac{Q_s}{1.4768 * 10^{-1} d^{3/2} \zeta \left(\frac{-(5/3)B}{A+(5/3)B}\right)^{5/3}} \tag{32}$$

Theoretically, the optimal width–depth ratio can encompass any positive integer greater than ζ_{mc}, implying that the range of the optimal width–depth ratio extends from ζ_{mc} to positive infinity. However, considering the practical constraints of river evolution, it is highly unlikely for a river's width–depth ratio to exceed 1000. Therefore, for mathematical analysis, this study posits an upper limit of the optimal width–depth ratio at 1000. Table 2 illustrates that the relative roughness of riverbanks to a riverbed (represented by λ) significantly influences the critical optimal width–depth ratio (ζ_{mc}). When λ is set to 0.1, the range of possible values for ζ_m spans from ζ_{mc} to 1000. Calculations revealed that

the variation range of τ_0/τ_c extended from 1 to 195.7 within this context. Similarly, when λ was set to 0.5, 1, and 2, with τ_0/τ_c varying within the same range, the corresponding variation range of ζ_m could be calculated. The results are presented in Table 3.

Table 3. Values and varying ranges of ζ_m when λ take various specific values.

λ	$\zeta_{m\max}$	Varying Range of ζ_m
0.1	1000	4~1000
0.5	833	3~833
1	625	3~625
2	215	2~215

The terms involving ζ_m in Formulas (29)–(32) are notably intricate. Mathematical transformations become imperative to streamline the computational process. For instance, when the relative roughness of riverbanks to a riverbed equals 1, a variation range for the optimal width–depth ratio ζ_m is established, ranging from 4 to 1000, with increments of 1.

An exponential fitting analysis of the terms dependent on ζ_m within Formulas (29)–(32) was performed using Excel. Consequently, the terms containing ζ_m in these formulas could be approximated by the following expressions:

$$\left(\frac{-(5/3)B}{A+(5/3)B}\right)^{65/9}\frac{A+(5/3)*B}{A}{\zeta_m}^2(\zeta_m+2)^{1/3} \approx 4*10^{-6}{\zeta_m}^{8.9069}, R^2 = 0.9986 \quad (33)$$

$$\left(\frac{-(5/3)B}{A+(5/3)B}\right)^{80/9}\zeta_m^2(\zeta_m+2)^{4/3} \approx 4*10^{-8}{\zeta_m}^{12.609}, R^2 = 0.9992 \quad (34)$$

$$\left(\frac{-(5/3)B}{A+(5/3)B}\right)^{5/3} \approx 0.0401*{\zeta_m}^{1.7444}, R^2 = 0.9982 \quad (35)$$

$$\left(\frac{-(5/3)B}{A+(5/3)B}\right)^{5/3}\zeta_m \approx 0.0401*{\zeta_m}^{2.7444}, R^2 = 0.9993 \quad (36)$$

Combining the terms of ζ_m contained in Equations (33)–(36) into Equations (29)–(32), could yield the following average hydraulic geometric relationship:

$$\begin{aligned} W &= 9.2753*10^5 d^{1.0769}(nQ)^{0.3916}Q_s^{0.1515} = 9.2753*10^{-5}(n)^{0.3916}\left(\frac{Q_s}{Q}\right)^{0.1515}Q^{0.5431} \\ D &= 0.0121*10^7 d^{1.6946}(nQ)^{0.6162}Q_s^{-0.3351} = 0.0121*10^7 d^{1.6946}(n)^{0.6162}\left(\frac{Q_s}{Q}\right)^{-0.3351}Q^{0.2811} \\ S_m &= 0.2172 d^{0.2148}(nQ)^{-0.8310}Q_s^{0.8005} = 0.2172 d^{0.2148}n^{-0.8310}\left(\frac{Q_s}{Q}\right)^{0.8005}Q^{-0.0305} \end{aligned} \quad (37)$$

The same methodology was employed to derive the average hydraulic geometric relationships for λ being the values of 0.5, 1, and 2, with the outcomes presented in Table 4. A comparative analysis of the hydraulic geometric relationships for these varying relative roughness values indicated that roughness n, sediment size d, flow discharge Q, and sediment discharge Q_s all exerted a substantial influence on the final equilibrium river width, depth, and specific gradient. To assess the relative impact of λ on these four variables, the exponential variation ranges of these variables in the four sets of average hydraulic geometric relationships were statistically compiled. The findings are the following:

$$\begin{aligned} W_m &= K_W d^{1.0769\sim1.1158}n^{0.3916\sim0.4058}\left(\frac{Q_s}{Q}\right)^{0.1207\sim0.1515}Q^{0.5265\sim0.5431} \\ D_m &= K_D d^{1.6684\sim1.6967}n^{0.6067\sim0.6170}\left(\frac{Q_s}{Q}\right)^{-(0.3368\sim0.3145)}Q^{0.2802\sim0.2922} \\ S_m &= K_s d^{0.2148\sim0.2577}n^{-(0.8310\sim0.8154)}\left(\frac{Q_s}{Q}\right)^{0.7667\sim0.8005}Q^{-(0.0487\sim0.0305)} \end{aligned} \quad (38)$$

Table 4. The averaged equilibrium hydraulic geometry when λ took various specific values.

λ	ζ_m	Averaged Equilibrium Channel Relationships
0.1	$4 \le \zeta_m \le 1000$	$W = 9.2753 * 10^5 d^{1.0769} (nQ)^{0.3916} Q_s^{0.1515} = 9.2753 * 10^{-5} d^{1.0769} (n)^{0.3916} \left(\frac{Q_s}{Q}\right)^{0.1515} Q^{0.5431}$
		$D = 0.0121 * 10^7 d^{1.6946} (nQ)^{0.6162} Q_s^{-0.3351} = 0.0121 * 10^7 d^{1.6946} (n)^{0.6162} \left(\frac{Q_s}{Q}\right)^{-0.3351} Q^{0.2811}$
		$S = 0.2172 d^{0.2148} (nQ)^{-0.8310} Q_s^{0.8005} = 0.2172 d^{0.2148} n^{-0.8310} \left(\frac{Q_s}{Q}\right)^{0.8005} Q^{-0.0305}$
0.5	$3 \le \zeta_m \le 833$	$W = 8.1486 * 10^5 d^{1.0772} (nQ)^{0.3916} Q_s^{0.1515} = 8.1486 * 10^5 d^{1.0772} n^{0.3916} \left(\frac{Q_s}{Q}\right)^{0.1515} Q^{0.5431}$
		$D = 0.0124 * 10^7 d^{1.6941} (nQ)^{0.6160} Q_s^{-0.3347} = 0.0124 * 10^7 d^{1.6941} (n)^{0.6160} \left(\frac{Q_s}{Q}\right)^{-0.3347} Q^{0.2813}$
		$S = 0.2905 d^{0.2209} (nQ)^{-0.8288} Q_s^{0.7957} = 0.2905 d^{0.2209} n^{-0.8288} \left(\frac{Q_s}{Q}\right)^{0.7957} Q^{-0.0331}$
1	$3 \le \zeta_m \le 265$	$W = 7.4526 * 10^5 d^{1.0773} (nQ)^{0.3918} Q_s^{0.1512} = 7.4526 * 10^5 d^{1.0773} (n)^{0.3918} \left(\frac{Q_s}{Q}\right)^{0.1512} Q^{0.5430}$
		$D = 0.0139 * 10^7 d^{1.6967} (nQ)^{0.6170} Q_s^{-0.3368} = 0.0139 * 10^7 d^{1.6967} (n)^{0.6170} \left(\frac{Q_s}{Q}\right)^{-0.3368} Q^{0.2802}$
		$S = 0.2269 d^{0.2159} (nQ)^{-0.8306} Q_s^{0.7996} = 0.2269 d^{0.2159} (n)^{-0.8306} \left(\frac{Q_s}{Q}\right)^{0.7996} Q^{-0.0310}$
2	$2 \le \zeta_m \le 215$	$W = 5.8931 * 10^5 d^{1.1158} (nQ)^{0.4058} Q_s^{0.1207} = 5.8931 * 10^5 d^{1.1158} n^{0.4058} \left(\frac{Q_s}{Q}\right)^{0.1207} Q^{0.5265}$
		$D = 0.0155 * 10^7 d^{1.6684} (nQ)^{0.6067} Q_s^{-0.3145} = 0.0155 * 10^7 d^{1.6684} n^{0.6067} \left(\frac{Q_s}{Q}\right)^{-0.3145} Q^{0.2922}$
		$S = 0.3152 d^{0.2577} (nQ)^{-0.8154} Q_s^{0.7667} = 0.3152 d^{0.2577} (n)^{-0.8154} \left(\frac{Q_s}{Q}\right)^{0.7667} Q^{-0.0487}$

In Equation (38), coefficients K_W, K_D, and K_S are correlation coefficients, respectively.

Equation (38) revealed that as the relative roughness values of riverbanks to a riverbed changed, specifically at 0.1, 0.5, 1, and 2, the coefficients of the four main variables—sediment discharge, flow discharge, roughness, and sediment size—within the formula exhibited minimal fluctuations. Consequently, these variable coefficients in Equation (38) could be approximated as constants in analyzing specific river geometries. When the values of λ were set to 0.1, 0.5, 1, and 2, the variation trends of the correlation coefficients K_W, K_D, and K_S in Equation (38) are depicted in Figure 3. It is evident that with an increase in the relative roughness of the riverbank to the riverbed, K_W experienced a gradual decrease, with values of 9.2753×10^5, 8.1486×10^5, 7.4526×10^5, and 5.8931×10^5 representing a decrease of up to 36.64%. Meanwhile, K_D gradually increased, with values of 0.0121×10^7, 0.0124×10^7, 0.0139×10^5, and 0.0155×10^7, respectively. However, K_S did not demonstrate a specific trend, with values ranging from 0.2172 to 0.2905, 0.2269, and 0.3152, respectively. This suggests that the coefficient K_S remains relatively stable or experiences minimal change and can thus be considered a constant. In summary, as the relative roughness of riverbanks to a riverbed increases, the river tends to adjust itself by adopting a wider and shallower cross-section for sediment transport and vice versa. However, the relative roughness of riverbanks to a riverbed has little influence on K_S, indicating a weak correlation between the two.

To facilitate a comparison with previous studies, we considered the energy gradient as an independent variable. By combining Formula (37) with Formula (1), we could derive hydraulic geometric relationships that related river width, river depth, flow velocity, roughness, flow, and energy gradient. These relationships are expressed as the following:

$$\begin{aligned} W_m &= 199.0 d^{-0.0407} (nQ)^{0.5489} S^{0.1893} \\ D_m &= 0.068 d^{0.0899} (nQ)^{0.2683} S^{-0.4186} \\ V_m &= 0.0739 d^{-0.0492} n^{-0.8172} Q^{0.1828} S^{0.2293} \end{aligned} \tag{39}$$

Similarly, the average hydraulic geometric relationships were derived for cases in which the relative roughness of riverbanks to a riverbed was set to 0.5, 1, and 2. These results are presented in Table 5. Upon comparing and analyzing the hydraulic geometric relationships across these different values of relative roughness, as shown in Table 4, it became evident that roughness, sediment size, flow discharge, and energy gradient all exerted a significant influence on the final equilibrium river width, depth, and velocity. To assess the degree of influence of λ on these four variables, we statistically summarized the exponential variation ranges of these variables across the four sets of average hydraulic geometric relationships. The results are the following:

$$\begin{aligned} W_m &= K'_W d^{-(0.0421\sim0.0406)} S^{0.1574\sim0.1904} (nQ)^{0.5188\sim0.5494} \\ D_m &= K'_D d^{0.0899\sim0.1057} S^{-(0.4212\sim0.4102)} (nQ)^{0.2671\sim0.2722} \\ V_m &= K'_V d^{-(0.0651\sim0.0492)} n^{-(0.8172-0.7910)} S^{0.2293-0.2528} Q^{0.1828\sim0.2090} \end{aligned} \tag{40}$$

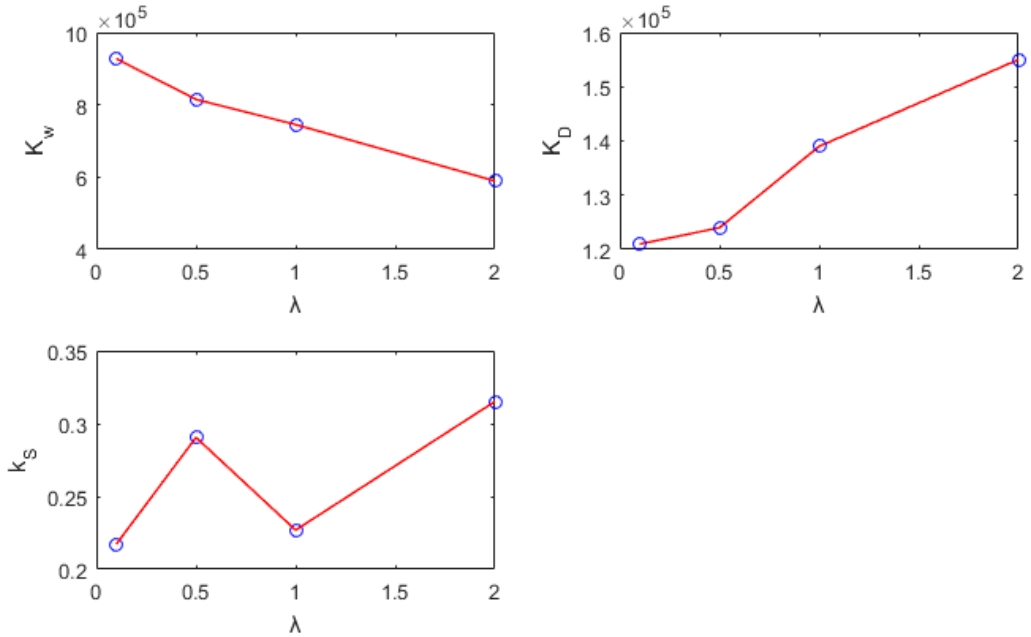

Figure 3. Relationships between coefficients K_W, K_D, and K_S in Equation (38) and λ.

Table 5. The averaged hydraulic geometry when λ took various specific values.

λ	ζ_m	Averaged Hydraulic Geometry Relationships
0.1	$4 \le \zeta_m \le 1000$	$W = 199.0d^{-0.0407}(nQ)^{0.5489}S^{0.1893}$ $D = 0.068d^{0.0899}(nQ)^{0.2683}S^{-0.4186}$ $V = 0.0739d^{-0.0492}n^{-0.8172}Q^{0.1828}S^{0.2293}$
0.5	$3 \le \zeta_m \le 833$	$W = 165.2629d^{-0.0421}(nQ)^{0.5494}S^{0.1904}$ $D = 0.0754d^{0.0929}(nQ)^{0.2674}S^{-0.4206}$ $V = 0.0803d^{-0.0508}n^{-0.8168}Q^{0.1832}S^{0.2302}$
1	$3 \le \zeta_m \le 625$	$W = 158.4510d^{-0.0408}(nQ)^{0.5489}S^{0.1891}$ $D = 0.0784d^{0.0909}(nQ)^{0.2671}S^{-0.4212}$ $V = 0.0805d^{-0.0501}n^{-0.8160}Q^{0.1840}S^{0.2321}$
2	$2 \le \zeta_m \le 215$	$W = 78.4891d^{-0.0406}(nQ)^{0.5188}S^{0.1574}$ $D = 0.1279d^{0.1057}(nQ)^{0.2722}S^{-0.4102}$ $V = 0.0996d^{-0.0651}n^{-0.7910}Q^{0.2090}S^{0.2528}$

In Equation (40), K_W, K_D, and K_S are correlation coefficients, respectively.

As indicated in Formula (40), when varying the values of the relative roughness of riverbanks to a riverbed at 0.1, 0.5, 1, and 2, the coefficients associated with the four key variables—namely, energy gradient, flow discharge, roughness, and sediment size in Formula (40)—exhibited only minimal fluctuations. Consequently, within the context of specific river geometry analysis, these coefficients within Formula (38) could be reasonably approximated as constants.

When we considered different values of λ, specifically 0.1, 0.5, 1, and 2, and examined the trends of the correlation coefficients K'_W, K'_D, and K'_V within Formula (40), a discernible pattern emerged (see Figure 4). As the relative roughness of riverbanks to a riverbed increased, coefficient K'_W exhibited a gradual decrease, with values of 199.0, 165.2629, 158.4510, and 78.4891, respectively. In contrast, coefficient K'_D displayed a progressive

increase, with values of 0.068, 0.0754, 0.0784, and 0.1279. Meanwhile, coefficient K'_V initially showed a slow increase followed by a more rapid rise, with values of 0.0739, 0.0803, 0.0805, and 0.0996, respectively. In broad terms, as the relative roughness of riverbanks to a riverbed diminishes, the river tends to adopt a wider and shallower cross-section for sediment transport and vice versa.

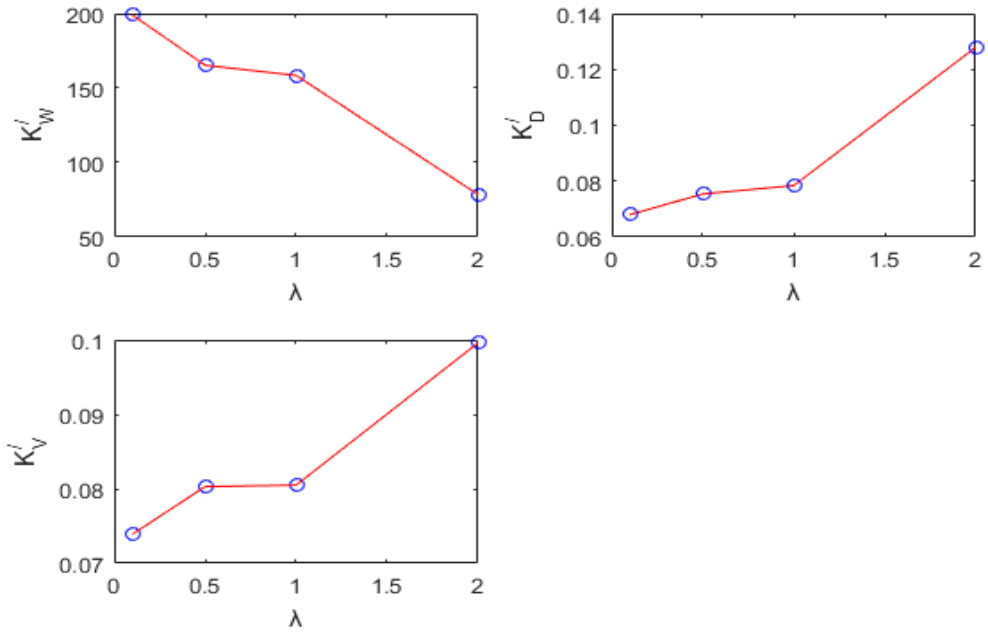

Figure 4. Relationships between coefficients K'_W, K'_D, and K'_V in Equation (40) and λ.

5. Comparative Analysis between This Study and Previous Studies

5.1. Hydraulic Geometric Relationships in the State of $\tau_0 = \tau_c$

Through a comparative analysis of the calculated hydraulic geometric relationship in the context of the critical incipient motion state with the classical threshold theoretical relationship and the prior study conducted by Fan and Huang [51], certain intriguing findings emerged. Notably, the flow discharge index in these relationships remained consistently near approximately 0.46. However, a notable disparity became evident in the critical optimal width–depth ratio obtained through the various methodologies, as detailed in Table 6. In the present study, the critical optimal width–depth ratio spanned a range of values between 1.62 and 3.12, while the results from Fan and Huang's study encompassed a range from 2 to 4. In stark contrast, the threshold theory, with its idealized assumptions, yielded a much broader range, spanning from 7.05 to 8.61. The principal reason for this discrepancy stems from the highly idealized conditions postulated by the threshold theory. Specifically, this theory assumes that all sediments within a river cross-section exist in a critical incipient motion, a condition that significantly deviates from the real-world complexities of river dynamics. This paper and Fan and Huang's (2020) study adopted a more nuanced approach, dividing the cross-section into two distinct components, the riverbank and the riverbed, each characterized by differing degrees of roughness [51]. Consequently, the theoretical outcomes derived from these studies align more closely with the observed sediment discharge in natural rivers, as documented by Nanson et al. (2010) [57]. Nevertheless, when comparing the results of this paper with those of Fan and Huang's research, it became apparent that the two river boundary anti-scourability factors introduced by the authors exerted a substantial influence on the ultimate equilibrium form of the river. To date, the collective impact of these factors, including the bank slope and relative roughness of a riverbank to a riverbed, on the eventual equilibrium configuration of the river, remains an unexplored avenue of inquiry. It is conceivable that should the combined influence of both factors be considered, the range of variation in the critical optimal width–depth ratio would likely expand. Moreover, it is reasonable to anticipate

that the range established by the threshold theory would fall within this broader spectrum. Nonetheless, the validity of such an assumption necessitates further research and empirical verification.

Table 6. Comparison among studies by Fan and Huang [51] and the "threshold theory" by Lane (1952) [58].

Channel Geometry Factor	This Study	Fan and Huang (2020) [51]	Threshold Theory (Lane, 1952) [58]
Width (W)	$W \propto Q^{0.46}$	$W \propto Q^{0.46}$	$W \propto Q^{0.46}$
Depth (D)	$D \propto Q^{0.46}$	$D \propto Q^{0.46}$	$D \propto Q^{0.46}$
Slope (S)	$S \propto Q^{-0.46}$	$S \propto Q^{-0.46}$	$S \propto Q^{-0.46}$
Width/depth ratio (W/D)	1.62–3.12	2–4	7.05–8.61

5.2. Hydraulic Geometric Relationships in the State of $\tau_0 > \tau_c$

Historically, flow discharge has been regarded as the primary controlling factor influencing river evolution. The development of "regime theory", based on observations of stable canals in countries such as India, Pakistan, and the United States, gained global recognition in the early 20th century [57]. However, a plethora of studies conducted on natural rivers have unveiled significant variations in the impact of flow discharge on river evolution, not only across different rivers but also within different sections of the same river. For instance, when examining hydraulic geometric relationships where flow discharge served as the primary variable (i.e., $W \propto Q^{l}$, $D \propto Q^{f}$ and $V \propto Q^{m}$), the exponents l, f, and m exhibited considerable variability, spanning the broad ranges of 0.3 to 0.6, 0.2 to 0.5, and 0.0 to 0.2, respectively [59]. In light of these disparities, numerous scholars have embarked on investigations into multivariable-dominated hydraulic geometric models. Notably, Huang and Warner (1995) formulated a comprehensive multivariable geometric model, drawing upon empirical formulas characterizing the distribution of shear forces across cross-sections in both natural rivers and stable canals [60]. This model is expressed as the following:

$$\begin{aligned} W &= C_W Q^{0.5} n^{0.355} S^{-0.156} \\ D &= C_D Q^{0.3} n^{0.383} S^{-0.206} \\ V &= C_V Q^{0.2} n^{0.383} S^{-0.206} \end{aligned} \tag{41}$$

In Equation (41), the coefficients C_W, C_D, and C_V represent correlation coefficients influenced primarily by the strength of riverbanks. Huang et al. conducted a comprehensive analysis of global river channel data and riverbank composition, using Formula (41) as the basis. Their research focused on evaluating the impact of riverbank strength on river channel evolution. Their findings revealed that changes in the composition of riverbanks can result in threefold variations in river width and roughly twofold changes in river depth.

Equation (41) demonstrates that, in addition to factors such as flow discharge, energy gradient, roughness, and bank strength, sediment size plays a significant role in shaping the hydraulic geometric relationship. Indeed, the influence of sediment size on river evolution has been substantiated by numerous prior empirical studies. In summary, this paper offers a comprehensive analysis of the various factors influencing river evolution. Notably, when factors such as the energy gradient, roughness, sediment size, and river boundary conditions are identical, or their influence on river evolution is minimal, the hydraulic geometric relationship can be simplified to a more elementary form, as illustrated in Table 7.

Table 7 presents the univariate hydraulic geometric relationship models explored in this paper alongside those developed by Fan, Rhodes, and Huang, respectively. It is evident that the flow discharge indices in these three hydraulic geometric relationships exhibit remarkable consistency, underscoring the sound reasoning and correctness of the arguments presented in this paper. Furthermore, although there exists a slight disparity in the range of flow index variation calculated in this paper compared to the authors' findings

in 2020, the range obtained in this paper aligns more closely with the flow index variations calculated by Huang and Warner (1995) [60].

Table 7. Comparison among the studies by Fan and Huang [51], Rhodes (1987) [59], and by Huang and Warner (1995) [60].

Hydraulic Geometry Factor	This Study	Fan and Huang (2020) [51]	Hydraulic Geometry Model (Rhodes, 1987) [59]	Huang and Warner (1995) [60]
Width (W)	$W \propto Q^{0.5188\sim0.5494}$	$W \propto Q^{0.5431\sim0.5489}$	$W \propto Q^{0.3\sim0.6}$	$W \propto Q^{0.5}$
Depth (D)	$D \propto Q^{0.2671\sim0.2722}$	$D \propto Q^{0.2655\sim0.2692}$	$D \propto Q^{0.2\sim0.5}$	$D \propto Q^{0.3}$
Velocity (V)	$V \propto Q^{0.1828\sim0.2090}$	$V \propto Q^{0.1840\sim0.1876}$	$V \propto Q^{0.0\sim0.3}$	$V \propto Q^{0.2}$

6. Discussion

The concept of river boundary conditions encompasses a multifaceted array of factors. While undoubtedly significant, the consideration of bank steepness may not comprehensively capture the entirety of riverbank anti-scourability. This recognition underscores the exigency of a more comprehensive investigation into the diverse factors contributing to a riverbank stability's complex dynamics. Such an exploration promises to yield more profound insights into the intricate evolutionary processes governing river geomorphology. Therefore, the current study examined a specific facet within this multifaceted realm: the relative roughness of riverbanks to a riverbed. Within this scholarly endeavor, a generalized cross-section of a river, characterized by a rectangular shape, was meticulously employed as a foundational element. This deliberate choice of configuration served as a lens through which to conduct an in-depth analysis of the profound influence exerted by the relative roughness of riverbanks to a riverbed on the ultimate equilibrium form of a river channel. Through a systematic deductive process, we sought to elucidate the critical and average hydraulic geometric relationships while considering various degrees of relative roughness about riverbanks and their interactions with riverbeds. These deduced relationships underwent rigorous scrutiny to ensure their consistency with prior theoretical analyses and empirical observations.

The pursuit of this investigation into the relative roughness of riverbanks to a riverbed constitutes a pivotal stride toward the augmentation of our understanding of river geomorphology. It promises to enrich our knowledge by shedding light on the intricate interplay between hydraulic factors and the critical concept of boundary anti-scourability within the context of river systems. This research encompasses an academic initiative with profound implications, offering the potential to enhance our grasp of river behavior and morphology, thus contributing to the effective management and conservation of these vital natural entities.

Nonetheless, it is imperative to underscore that the scope of this investigation remained confined to theoretical analysis. Applying these theoretical insights to the practical analysis of river morphological evolution warrants further in-depth research. This transition from theoretical constructs to empirical application necessitates a nuanced examination to ensure that the proposed theoretical framework aligns seamlessly with the intricate realities of specific river systems. Consequently, future research endeavors should endeavor to bridge this gap, thus facilitating the practical utilization of these findings in the comprehensive assessment of river morphology and its evolution.

Moreover, the quantitative determination of the relative roughness of riverbanks to a riverbed within the context of individual rivers emerged as a distinct avenue for future exploration. The complexity of river systems, with their unique hydraulic conditions, sediment compositions, and environmental influences, necessitates tailored approaches for quantification. To this end, a systematic investigation is warranted to devise robust methodologies for precisely and quantitatively characterizing the relative roughness of riverbanks to a riverbed in the context of specific rivers. This endeavor is pivotal for enhancing the accuracy and applicability of geomorphological assessments of rivers, thereby contributing to a more comprehensive understanding of the intricate interplay between

hydraulic factors and boundary anti-scourability within river systems. Furthermore, this quantitative determination has the potential to serve as a valuable tool for river management and conservation efforts, enabling a more tailored and effective approach to the preservation and restoration of these vital natural systems.

7. Conclusions

Numerous prior empirical investigations have delved into the ramifications of bank anti-scourability on river channel morphology. Nevertheless, utilizing a physical mechanism model for a comprehensive quantification of this impact has been a relatively underexplored avenue within the existing body of literature. Drawing upon Huang's equilibrium theory and employing the variational analysis method, this study endeavored to shed light on this facet by employing a rectangular cross-section to represent a river and designating the relative roughness of riverbanks to a riverbed as λ to denote the robustness of the riverbanks. The theoretical scrutiny of the influence of the relative roughness of riverbanks to a riverbed on the equilibrium channel configuration of an alluvial river yielded several noteworthy findings:

Primarily, it was observed that for any given value of λ, there exist a unique parameter, namely, the optimal width–depth ratio of the sediment transport section. This implies that at this juncture, the sediment discharge across the river cross-section attains its maximum capacity. In essence, any deviation from this critical value, be it an increase or decrease in the width–depth ratio, results in a diminished sediment discharge for the river. Furthermore, it was ascertained that as the value of λ transitions from smaller to larger magnitudes, the calculated maximum sediment discharge experiences a reduction while the optimal width–depth ratio undergoes an expansion. This discernment underscores the phenomenon that as the relative roughness of riverbanks to a riverbed intensifies, the river tends to exhibit a broader and shallower cross-section for the transportation of sediment.

Secondly, in the scenario where river sediment was in a critical incipient motion state, denoted by $\tau_0 = \tau_c$, the univariate hydraulic geometric relationship proposed in this study closely resembled that which is conventionally computed using the classic "threshold theory".

Thirdly, under certain circumstances, when variables such as the energy gradient, channel roughness, sediment size, bank angle, and relative roughness of riverbanks to a riverbed can be approximated as constants, exerting a negligible influence on a river's evolutionary trajectory, the multivariable hydraulic geometric relationship articulated in this study can be elegantly simplified into a univariate model contingent upon flow discharge. This streamlined model exhibits a high degree of concordance with previous research endeavors.

Lastly, as the parameter λ underwent a progression from relatively small values to larger magnitudes, specifically adopting values of 0.1, 0.5, 1, and 2, a nuanced analysis of the indices pertaining to variables encompassing flow discharge, energy gradient, channel roughness, and sediment size revealed remarkably limited fluctuations, rendering them nearly akin to constant values. Simultaneously, this variation in λ manifested itself in a notable reduction in river width by as much as 36.46%, coupled with a concomitant elevation in river depth by as much as 28%.

Rivers, in conjunction with various geomorphic agents, play a pivotal role in shaping landscapes through erosional processes and the transportation of detritus and sediments. These dynamic watercourses exhibit inherent physical characteristics that facilitate self-adjustment in response to a multitude of environmental factors. The variational method, recognized for its efficacy in providing a physical framework for analyzing river dynamics, emerged as an invaluable tool in this context. This paper, leveraging the variational method, endeavored to formulate a comprehensive multivariable hydraulic geometric model that took into account the influence of river boundary conditions. Within this model, the intricate interplay of multiple variables was examined, shedding light on the complex river evolution process under the influence of these multivariable factors.

It is essential to emphasize, however, that the focus of this inquiry remained centered on theoretical analysis. The transition from these theoretical constructs to their practical application in the realm of river morphological evolution necessitates further in-depth research. The quantification of the relative roughness of riverbanks to a riverbed in the specific context of individual rivers emerged as a distinctive avenue for future exploration. This quantitative determination enriches our understanding of the complex interplay of variables within the intricate world of river dynamics and offers promising insights into real-world applications.

Author Contributions: Conceptualization, J.F. and X.L.; methodology, J.F. and X.L.; software, J.F.; validation, J.F., Q.L., Y.B., X.L. and R.L.; formal analysis, J.F. and X.L.; investigation, J.F., X.L. and R.L.; resources, J.F. and X.L.; data curation, J.F.; writing—original draft preparation, J.F.; writing—review and editing, J.F., Q.L., Y.B. and X.L.; visualization, J.F., Q.L., Y.B. and X.L.; supervision, J.F., Q.L., Y.B. and X.L.; funding acquisition, J.F. All authors have read and agreed to the published version of the manuscript.

Funding: This research was financially supported by the independent scientific research projects of Yellow River Engineering Consulting Co., Ltd. (2021BSHZL03).

Data Availability Statement: Data are contained within the article.

Conflicts of Interest: Authors Jinsheng Fan and Qiushi Luo were employed by the company Yellow River Engineering Consulting Co., Ltd. and author Xiaofang Liu was employed by the company Beijing Capital Ecological Environmental Protection Group Co., Ltd. The remaining authors declare that the research was conducted in the absence of any commercial or financial relationships that could be construed as a potential conflict of interest.

References

1. Blench, T. *Mobile Bed Fluviology*; University of Alberta Press: Edmonton, AB, Canada, 1969; 164p.
2. Mackin, J. Concept of the gradedriver. *GSA Bull.* **1948**, *59*, 463. [CrossRef]
3. Gray, W.G.; Ghidaoui, M.S.; Karney, B.W. Does the stream power theory have a physical foundation? *J. Hydraul. Res.* **2018**, *56*, 585–595. [CrossRef]
4. Nanson, G.C.; Huang, H.Q. Least action principle, equilibrium states, iterative adjustment and the stability of alluvial channels. *Earth Surf. Process. Landf.* **2008**, *33*, 923–942. [CrossRef]
5. Nanson, G.C.; Huang, H.Q. Self-adjustment in rivers: Evidence for least action as the primary control of alluvial-channel form and process. *Earth Surf. Process. Landf.* **2017**, *42*, 575–594. [CrossRef]
6. Nanson, G.C.; Huang, H.Q. A philosophy of rivers: Equilibrium states, channel evolution, teleomatic change and least action principle. *Geomorphology* **2018**, *302*, 3–19. [CrossRef]
7. Lane, E.W. The design of stable channels. *Trans. ASEC* **1955**, *120*, 1234–1279. [CrossRef]
8. Huang, H.Q.; Nanson, G.C. Vegetation and channel variation; A case study of four small streams in southeastern Australia. *Geomorphology* **1997**, *18*, 237–249. [CrossRef]
9. Huang, H.Q.; Nanson, G.C. The influence of bank strength on channel geometry: An integrated analysis of some observations. *Earth Surf. Process. Landf.* **1998**, *23*, 865–876. [CrossRef]
10. Hey, R.D.; Thorne, C.R. Stable channels with mobile gravel beds. *J. Hydraul. Eng.-ASCE* **1986**, *112*, 671–689. [CrossRef]
11. Lacey, G. Stable channels in alluvium. *Proc. Inst. Civ. Eng.* **1929**, *229*, 259–292.
12. Andrews, E.D. Bed-material entrainment and hydraulic geometry of gravel-bed rivers in Colorado. *Bull. Geol. Soc. Am.* **1984**, *95*, 371–378. [CrossRef]
13. Leopold, L.B.; Wolman, M.G. River channel patterns—Braided, meandering and straight. *Prof. Geogr.* **1957**, *9*, 39–85.
14. Schumm, S.A. *Geomorphic Thresholds and the Complex Response of Drainage System, Fluvial Geomorphology*; Publications of Geomorphology; State University of New York: New York, NY, USA, 1973; pp. 299–310.
15. Schumm, S.A. *The Fluvial System*; A Wiley-Interscience Publication: Hoboken, NJ, USA, 1977.
16. Schumm, S.A. *Experimental Fluvial Geomorphology*; John Wiley & Sons: Hoboken, NJ, USA, 1987.
17. Schumm, S.A.; Khan, H.R. Experimental study of channel patterns. *GSA Bull.* **1972**, *83*, 1755. [CrossRef]
18. Huang, H.Q.; Nanson, G.C. Hydraulic geometry and maximum flow efficiency as products of the principle of least action. *Earth Surf. Process. Landf.* **2000**, *25*, 1–16. [CrossRef]
19. Parker, G. Self-formed straight rivers with equilibrium banks and mobile bed, 1, the sand-silt river. *J. Fluid Mech.* **1978**, *89*, 109–125. [CrossRef]
20. Parker, G. Self-formed straight rivers with equilibrium banks and mobile bed, 2, the gravel river. *J. Fluid Mech.* **1978**, *89*, 127–146. [CrossRef]
21. Ikeda, S.; Parker, G.; Kimura, Y. Stable width and depth of straight gravel rivers with hetrogeneous bed materials. *Water Resour. Res.* **1988**, *24*, 713–722. [CrossRef]

22. Chang, H.H. Geometry of rivers in regime. *J. Hydraul. Div. ASCE* **1979**, *105*, 691–706. [CrossRef]
23. Chang, H.H. Minimum stream power and river channel patterns. *J. Hydrol.* **1979**, *41*, 303–327. [CrossRef]
24. Chang, H.H. Geometry of gravel streams. *J. Hydraul. Div. ASCE* **1980**, *106*, 1443–1456. [CrossRef]
25. Chang, H.H. Stable alluvial canal design. *J. Hydraul. Div. ASCE* **1980**, *106*, 873–891. [CrossRef]
26. Chang, H.H. Mathematical-model for erodible channels. *J. Hydraul. Div. ASCE* **1982**, *108*, 678–689. [CrossRef]
27. Chang, H.H. Analysis of river meanders. *J. Hydraul. Div. ASCE* **1984**, *110*, 37–50. [CrossRef]
28. Chang, H.H. Modeling of river channel changes. *J. Hydraul. Div. ASCE* **1984**, *110*, 157–172. [CrossRef]
29. Chang, H.H. River morphology and thresholds. *J. Hydraul. Div. ASCE* **1985**, *111*, 503–519. [CrossRef]
30. Mengoni, B.; Paris, E.; Bettess, R. Analytical approach to river regime. *J. Hydraul. Div. ASCE* **1982**, *108*, 1179–1193.
31. Yang, C.T. Unit stream power and sediment transport. *J. Hydraul. Div. ASCE* **1974**, *100*, 1269–1272. [CrossRef]
32. Yang, C.T. Minimum unit stream power and fluvial hydraulics. *J. Hydraul. Div. ASCE* **1976**, *102*, 919–934. [CrossRef]
33. Yang, C.T. Closure to Minimum unit stream power and fluvial hydraulics. *J. Hydraul. Div. ASCE* **1978**, *104*, 122–125. [CrossRef]
34. Yang, C.T. Unit stream power equations for total load. *J. Hydrol.* **1979**, *40*, 123–138. [CrossRef]
35. Yang, C.T. Unit stream power equation for gravel. *J. Hydraul. Div. ASCE* **1984**, *110*, 1783–1797. [CrossRef]
36. Yang, C.T.; Molinas, A. Sediment transport and unit stream power function. *J. Hydraul. Div. ASCE* **1982**, *108*, 774–793. [CrossRef]
37. Yang, C.T.; Song, C.C.S. Theory of minimum rate of energy-dissipation. *J. Hydraul. Div. ASCE* **1979**, *105*, 769–784. [CrossRef]
38. Yang, C.T.; Song, C.C.S.; Woldenberg, M.J. Hydraulic geometry and minimum rate of energy-dissipation. *Water Resour. Res.* **1981**, *17*, 1014–1018. [CrossRef]
39. Yang, C.T.; Stall, J.B. Applicability of unit stream power equation-closure. *J. Hydraul. Div. ASCE* **1978**, *104*, 1095–1103. [CrossRef]
40. Eaton, B.C.; Millar, R.G. Optimal alluvial channel width under a bank stability constraint. *Geomorphology* **2004**, *62*, 35–45. [CrossRef]
41. Song, C.C.S.; Yang, C.T. Comment on "Extremal hypotheses for river regime: An illsion of progress" by George A. Griffiths. *Water Resour. Res.* **1986**, *22*, 993–994. [CrossRef]
42. Ferguson, R.I. Hydraulics and hydraulic geometry. *Prog. Phys. Geogr. Earth Environ.* **1986**, *10*, 1–31. [CrossRef]
43. Griffiths, G.A. Extremal Hypotheses for River Regime: An Illusion of Progress. *Water Resour. Res.* **1984**, *20*, 113–118. [CrossRef]
44. Chang, H.H. Comment on "Extremal hypotheses for river regime: An illusion of progress" by George A. Griffiths. *Water Resour. Res.* **1984**, *20*, 1767–1768. [CrossRef]
45. Millar, R.G. Theoretical regime equations for mobile gravel-bedrivers with stable banks. *Geomorphology* **2005**, *64*, 207–220. [CrossRef]
46. Eaton, B.; Millar, R. Predicting gravel bed river response to environmental change: The strengths and limitations of a regime-based approach. *Earth Surf. Process. Landf.* **2017**, *42*, 994–1008. [CrossRef]
47. Huang, H.Q.; Nanson, G.C. A stability criterion inherent in laws governing alluvial channel flow. *Earth Surf. Process. Landf.* **2002**, *27*, 929–944. [CrossRef]
48. Huang, H.Q.; Chang, H.H.; Nanson, G.C. Minimum energy as the general form of critical flow and maximum flow efficiency and for explaining variations in river channel pattern. *Water Resour. Res.* **2004**, *40*, 13. [CrossRef]
49. Huang, H.Q.; Nanson, G.C. Why some alluvial rivers develop an anabranching pattern. *Water Resour. Res.* **2007**, *43*, 12. [CrossRef]
50. Huang, H.Q. Reformulation of the bed load equation of Meyer-Peter and Muller in light of the linearity theory for alluvial channel flow. *Water Resour. Res.* **2010**, *46*, 11. [CrossRef]
51. Fan, J.; Huang, H.; Yu, G.; Su, T. River channel forms in relation to bank steepness: A theoretical investigation using a variational analytical method. *Water* **2020**, *12*, 1250. [CrossRef]
52. Manning, R. On the Flow of Water in Open Channels. *Trans. Inst. Civ. Eng. Irel.* **1889**, *20*, 161–207.
53. Chien, N. *Meyer-Peter Formula for Bed Load Transport Aniond Einstein Bed Load Function*; University of California: Berkeley, CA, USA, 1954.
54. Meyer-Peter, E.; Muller, R. Formulas for Bed-Load Transport. In *IAHSR 2nd Meeting, Stockholm, Appendix 2*; IAHR: Madrid, Spain, 1948.
55. Einstein, H.A. Formula for transportation of bed load. *Trans. ASEC* **1942**, *107*, 561–597. [CrossRef]
56. Einstein, H.A. *The Bed Load Function for Sediment Transportation in Open Channel Flows*; Technical Bulletin; U.S. Department of Agriculture: Washington, DC, USA, 1950; p. 71.
57. Nanson, R.A.; Nanson, G.C.; Huang, H.Q. The hydraulic geometry of narrow and deep channels: Evidence for flow optimisation and controlled peatland growth. *Geomorphology* **2010**, *117*, 143–154. [CrossRef]
58. Lane, E.W. *Progress Report on Results of Studies on Design of Stable Channels*; Hydraulic Laboratory Report Hyd-352; U.S. Bureau of Reclamation: Washington, DC, USA, 1952.
59. Rhodes, D.D. The b-f-m diagram for downstream hydraulic geometry. *Geogr. Ann. Ser. A Phys. Geogr.* **1987**, *69*, 147. [CrossRef]
60. Huang, H.Q. The multivariate controls of hydraulic geometry: A causal investigation in terms of boundary shear distribution. Earth Surf. Process. *Landforms* **1995**, *20*, 115–130. [CrossRef]